MgB$_2$ single crystals substituted with Li and with Li-C: Structural and superconducting properties

J. Karpinski,[1,*] N. D. Zhigadlo,[1] S. Katrych,[1] K. Rogacki,[1,2] B. Batlogg,[1] M. Tortello,[1,3] and R. Puzniak[1,4]

[1]*Laboratory for Solid State Physics, Eidgenössische Technische Hochschule, 8093 Zurich, Switzerland*
[2]*Institute of Low Temperature and Structure Research, Polish Academy of Sciences, P.O. Box 1410, 50-950 Wroclaw, Poland*
[3]*Dipartimento di Fisica and CNISM, Politecnico di Torino, 10129 Torino, Italy*
[4]*Institute of Physics, Polish Academy of Sciences, Aleja Lotnikow 32/46, 02-668 Warsaw, Poland*

The effect of Li substitution and Li-C co-substitution on the superconducting properties and crystal structure of MgB$_2$ single crystals has been investigated. Hole doping with Li decreases the superconducting transition temperature T_c at a slower rate than that of the electron doping with C or Al. For crystals co-substituted with Li for Mg and C for B, T_c decreases more rapidly than for crystals substituted with C alone. This means that holes introduced with Li cannot counterbalance the influence of electrons doped with C and are not able to prevent T_c to decrease. The possible explanation is that holes coming from Li occupy mainly the π band while electrons coming from C fill the σ band. The resistivity in both Li substituted and Li-C co-substituted crystals is significantly increased, reflecting scattering due to substitutional defects, including distortion of the lattice. Li substitution decreases the upper critical field $H_{c2}(T)^{\|ab}$ while $H_{c2}(T)^{\|c}$ does not change. The temperature dependences of H_{c2} for the Li and Al single-substituted crystals with the same T_c show a similar $H_{c2}(T)$ behavior despite the different substitution level.

PACS number(s): 74.70.Ad, 74.62.Dh, 81.10.−h, 74.25.Ha

I. INTRODUCTION

After several years of intensive investigations, the superconducting and normal state properties of pure MgB$_2$ are now well explored by experiment and are explained by theory. MgB$_2$ is a two-band two-gap superconductor with several anomalous properties originating from the existence of two separate sheets of the Fermi surface (FS): first one is a quasi-two-dimensional FS related to the σ band and a second sheet is three-dimensional formed by the π states.[1–5] This peculiar electronic structure and strong electron-phonon coupling, predominantly in the σ sheet, lead to the high critical temperature T_c of 39 K and to a pronounced temperature and field dependent anisotropy of electronic properties, particularly in the superconducting state.[6–8] The evolution of the two gaps as a function of temperature and field has been studied in detail by a point contact spectroscopy[9–11] and by a scanning tunneling spectroscopy.[12–14]

The critical temperature and other superconducting properties of a two-band superconductor depend on the doping level and on the interband and intraband scattering.[15–17] These properties can be modified by chemical substitutions, which change the electronic and defect structures, and thus, the superconducting gaps and the interband and intraband scattering. A potential practical interest would be an enhancement of the upper critical field H_{c2} and a reduction of its anisotropy. However, the understanding of the modifications of these parameters by chemical substitutions is still emerging. In order to study the influence of doping and intraband and interband scattering on the gap and other superconducting properties, investigations of partially substituted MgB$_2$ are of particular interest. Due to the anisotropic character of MgB$_2$, single crystal studies provide a more detailed insight and such studies have been reported for C, Al, and Mn substitutions.[18–23] Other substitutions, such as Li[24,25] and

Mn substitutions[26,27] were investigated on polycrystalline samples or polycrystalline thin films.

Carbon substituted for boron produces particularly pronounced modifications: the upper critical fields for both orientations, $H_{c2}^{\|ab}$ and $H_{c2}^{\|c}$, increase with an associated decrease of the H_{c2} anisotropy, $H_{c2}^{\|ab}/H_{c2}^{\|c}$.[20,28,29] This has been explained as a result of the reduced mean free path due to enhanced intraband scattering in the σ band.[20,30–32] Both the C substitution for B and the Al substitution for Mg add electrons to MgB$_2$. Theory predicts the merging of both gaps with increased interband scattering caused by substitution.[5,17] Such an effect was confirmed experimentally for MgB$_2$ crystals with 13% C substitution.[33] However, merging of the gaps was not observed in polycrystalline samples synthesized at lower temperature and normal pressure, under conditions which may result in the different amount and structure of the substitution-induced defects and thus, in different interband scattering.[34] According to Kortus *et al.*,[5] stronger interband scattering is expected for the C substitution because the σ band orbitals are located in the B plane and there is not much weight of the σ band in the Mg plane. The π orbitals are also centered in the B plane, however, they extend further out toward the Mg plane. For these reasons, impurities in the B plane are much more effective interband scatterers than the impurities in the Mg plane. The decrease of T_c with Al or C substitution has been attributed to σ hole-band filling and, in the case of the C substitution, partially to the increase of the interband scattering. Both Al and C (when dope with electrons) reduce the number of holes at the top of the σ band together with the reduction in the electronic density of states, and thus, both decrease T_c in a similar way. Mn is found to substitute isovalently for Mg with a magnetic moment strongly interacts with the conduction electrons. This leads to pair breaking and strong suppression of superconductivity ($T_c=0$ for 2% of Mn) and anisotropy.[22]

Hole doping in MgB_2 has been investigated very little and only few papers concerned polycrystalline MgB_2:Li have been published.[24,25] Co-doping with holes and electrons is a very interesting issue because it can widen the possibility to tune the electronic band doping and the intraband and interband scattering.[5] In the crystals where Li and C or Li and Al are substituted simultaneously, one can expect some compensation of the electron doping effect and an increase of T_c. Two papers have been published on the Al-Li co-substitution in polycrystalline samples.[26,27] Xu *et al.*[26] found a substantial influence of Li on T_c, but Monni *et al.*[27] showed that at up to 15% of substituted Li, T_c depends only on the content of Al. Bernardini *et al.*[35] calculated the effect of the Li-Al co-substitution on the electronic structure and concluded that the holes added by Li go almost entirely to the π band and, thus, do not counterbalance the electron donation from Al, which fill the σ band. In such a case, the observed changes in T_c can be attributed to the effect of σ band filling only.

In this paper, we present the effect of the Li substitution for Mg and of the Li-C co-substitution on the superconducting properties and structure of MgB_2 single crystals. The objectives of these studies are twofold. First, we investigate the influence of Li^{+1} substitution on T_c, structure, H_{c2}, and its anisotropy. We will show that the hole doping with Li decreases T_c at a slower rate than electron doping with C or Al. Second, we study the role played by Li in the Li-C co-substituted crystals and a possible counterbalance effect of the simultaneous hole and electron doping. Such effect could have a practical importance because it might prevent T_c to decrease without losing the benefit of increased H_{c2} due to the C substitution. We will show that the influence of the Li-C co-substitution on T_c is different from that observed for the Li-Al substitution[26,27,35] and that Li added to C-substituted MgB_2 decreases T_c additionally.

II. EXPERIMENT

Single crystals of $Mg_{1-x}Li_x(B_{1-y}C_y)_2$ were grown under high pressure using the cubic anvil press. The applied pressure and temperature conditions for the growth of MgB_2 single crystals were determined in our earlier study of the Mg-B-N phase diagram.[36,37] Magnesium (Fluka, 99.99% purity), amorphous boron (Alfa Aesar, >99.99%), carbon graphite powder (Alfa Aesar, >99.99%), and lithium nitride (Alfa Aesar, >99.5%) were used as starting materials. Amorphous boron was annealed under dynamic vacuum at 1200 °C to minimize the contamination by oxygen. Due to the extremely hydroscopic nature of lithium nitride, starting materials with various nominal contents were mixed and pressed in a glove box. A pellet was put into a BN container of 8 mm inner diameter and 8.5 mm length. The heating element was a graphite tube. Six anvils generate pressure on the whole assembly. Lithium and Li-C substituted crystals were grown in the same way as the unsubstituted crystals.[36,37] First, a 30 kbar pressure was applied using a pyrophylite pressure transmitting cube as a medium and then the temperature was increased for one hour up to the maximum range of 1900–1950 °C, kept for 30 min, and decreased during 1–2 h. We obtained Li substituted and double
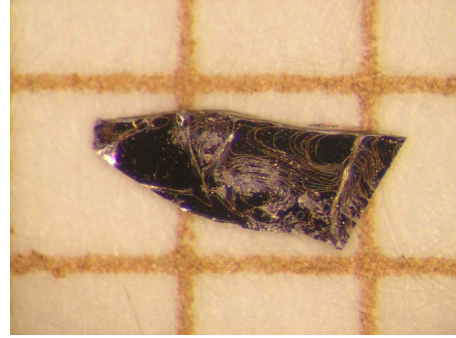
FIG. 1. (Color online) MgB_2 crystal substituted with Li. Scale is 1 mm.

Li and C co-substituted MgB_2 single crystals with dimensions up to $1.5 \times 0.8 \times 0.1$ mm^3 (Fig. 1). Crystals substituted with C were black in color, in contrast to crystals substituted with Li or unsubstituted, which were golden.

The crystal structure was investigated on single crystal x-ray Xcalibur PX Oxford Diffraction (at the Laboratory of Crystallography, ETHZ) and Siemens P4 diffractometers. The unit cell parameters were estimated for each sample from the same set of 32 reflections in the 20–40 deg wide 2Θ range. Data reduction and the analytical absorption correction were introduced using the CRYSALIS software package.[38] The carbon content in the crystals was estimated from the changes in the *a* lattice parameter. The lithium content was determined from structure refinement. Details of the structure investigations are described in the following chapter. In order to determine T_c, the magnetic moment of an individual crystal was measured at 0.1–0.5 mT field on a homemade superconducting quantum interference device magnetometer with a Quantum Design sensor. The magnetic measurements of the upper critical field were performed on a Quantum Design magnetic property measurement system with a 7 T magnet. Resistivity measurements were carried out in a Quantum Design physical property measurement system with a 14 T magnet using a standard four-point probe technique.

III. RESULTS AND DISCUSSION

A. Single-crystal structure analysis

The Li content was estimated using a refinement on F^2.[39] Theoretical calculations indicate that only 0.75 of the magnesium atoms per formula unit are needed to provide the chemical bonding in $Mg_{0.96}B_2$ (Ref. 40). The rest of the atoms $(0.96-0.75=0.21)$ gives additional electrons responsible for covalent interactions between magnesium and boron atoms along [001] direction.[41] We have assumed that lithium ions occupy the Mg site and provide fewer electrons than the Mg ions. The sum of both cations was increased to 100% and their occupations were refined. The positions and atomic displacement parameters for both cations were held to be equal (restrained). The refinement data are presented in Tables I and II. With the assumption of 100% sites occupation, the estimated standard deviations of the lithium concentration were about 1–1.5%. Because we do not have independent

TABLE I. Structure refinement and crystal data for MgB$_2$ and for MgB$_2$ doped with Li.

Sample	AN310/2	AN407/2	AN453/5	AN453/7
Empirical formula	Mg$_{0.98}$B$_2$	Mg$_{0.95}$Li$_{0.05}$B$_2$	Mg$_{0.90}$Li$_{0.10}$B$_2$	Mg$_{0.89}$Li$_{0.11}$B$_2$
$T_{c,on}$ (K)	38.5	38.5	35.6	35.8
T_c (K)	38.4	38.25	35.55	35.3
Formula weight	45.44	45.06	44.19	44.02
Temperature (K)		295(2)		
Wavelength (Å)/radiation		0.71073/Mo $K\alpha$		
Cell determined on		Siemens P4 four circles diffractometer (point detector)		
2Θ range for cell determination (deg)		31,1		
Intensity collection on diffractometer		Oxford diffraction four circles diffractometer (CCD detector)		
Crystal system (space group)		Hexagonal ($P6/mmm$)		
Unit cell dimensions (Å)	a=3.0875(5), c=3.5239(2)	a=3.0837(4), c=3.5176(6)	a=3.0828(8), c=3.512(1)	a=3.0826(5), c=3.5109(8)
Unit cell volume (Å^3)	29.09(1)	28.968(7)	28.91(2)	28.89(1)
Z		1		
Calculated density (g/cm^3)	2.595	2.584	2.539	2.531
Absorption correction type		Analytical		
Absorption coefficient (mm^{-1})	0.603	0.592	0.560	0.555
F(000)	22	22	21	21
Crystal size, mm	0.27×0.20×0.04	0.26×0.11×0.03	0.27×0.11×0.03	0.16×0.11×0.005
Θ range for data collection (deg)	7.65–36.06	5.80–30.34	5.81–36.08	5.81–30.11
Limiting indices	$-5 \leq h \leq 4$, $-3 \leq k \leq 5$, $-5 \leq l \leq 3$	$-4 \leq h \leq 4$, $-4 \leq k \leq 4$, $-4 \leq l \leq 5$	$-5 \leq h \leq 5$, $-5 \leq k \leq 5$, $-5 \leq l \leq 5$	$-4 \leq h \leq 4$, $-4 \leq k \leq 3$, $-4 \leq l \leq 3$
Reflections collected/unique	440/45, R$_{int}$=0.0186	477/33, R$_{int}$=0.0423	1017/46, R$_{int}$=0.0336	269/31, R$_{int}$=0.0212
Max. and min. transmissions	0.979 and 0.892	0.956 and 0.834	0.974 and 0.870	0.989 and 0.902
Refinement method		Full-matrix least squares on F^2		
Data/restraints/parameters	45/0/6	33/0/6	46/0/6	31/0/6
Goodness of fit on F^2	0.999	1.202	1.173	1.286
Final R indices [$I > 2\sigma(I)$]	R_1=0.0176, wR_2=0.0426	R_1=0.0306, wR_2=0.0778	R_1=0.0233, wR_2=0.0585	R_1=0.0183, wR_2=0.0540
R indices (all data)	R_1=0.0195, wR_2=0.0429	R_1=0.0309, wR_2=0.0778	R_1=0.0278, wR_2=0.0590	R_1=0.0196, wR_2=0.0542
$\Delta\rho_{max}$ and $\Delta\rho_{min}$, (e/Å^3)	0.293 and -0.202	0.216 and -0.461	0.299 and -0.289	0.203 and -0.222

prove that Li fills all Mg vacancies, it is possible that both Li atoms and Mg vacancies are present on Mg sites. Figure 2 shows the variation of the lattice parameters with Li content. The lattice parameter c decreases with Li substitution while a appears to remain essentially constant except for an initial decrease at low Li concentrations. The carbon content in Li-C co-substituted crystals was estimated from the changes of the lattice parameter a, assuming the linear dependence of the a parameter on the carbon content, according to the data of Avdeev *et al.*,[42] and by taking into account the small decrease of the a due to the presence of Li. We assumed that C

substitutes only for B. The occupations of anion sites were held constant with the sum of both anions equal to 100%. The positions and atomic displacement parameters of both anions were held to be equal (restrained).

The two-dimensional profiles of the (002) reflection for samples with various compositions (MgB$_2$, Mg$_{0.89}$Li$_{0.11}$B$_2$, Mg$_{0.89}$Li$_{0.11}$B$_{1.88}$C$_{0.12}$, and Mg$_{0.90}$Li$_{0.10}$B$_{1.85}$C$_{0.15}$) were constructed from the 30–40 one-dimensional scans using P4 Siemens diffractometer (Fig. 3). In pure, as well as in Li substituted MgB$_2$, the reflection profiles are narrow in the direction perpendicular to the c^* axis but elongated along b^*

TABLE II. Structure refinement and crystal data for MgB_2 substituted with Li and C.

Sample	AN467/1	AN456/6	AN456/10	AN456/4
Empirical formula	$Mg_{0.94}Li_{0.06}B_{1.96}C_{0.04}$	$Mg_{0.91}Li_{0.09}B_{1.84}C_{0.16}$	$Mg_{0.90}Li_{0.10}B_{1.82}C_{0.18}$	$Mg_{0.89}Li_{0.11}B_{1.88}C_{0.12}$
$T_{c,on}$, (K)	35.8	30.6	28.9	30.2
T_c, (K)	35.6	30.15	28.5	29.9
Formula weight	44.94	44.56	44.41	44.16
Temperature, (K)		295(2)		
Wavelength (Å)/radiation		0.71073/Mo $K\alpha$		
Cell determined on		Siemens P4 four circles diffractometer (point detector)		
2Θ range for cell determination (deg)		31,1		
Intensity collection on diffractometer		Oxford diffraction four circles diffractometer (CCD detector)		
Crystal system (space group)		Hexagonal ($P6/mmm$)		
Unit cell dimensions (Å)	$a=3.075(2)$, $c=3.522(3)$	$a=3.0561(6)$, $c=3.5190(10)$	$a=3.053(1)$, $c=3.522(2)$	$a=3.0602(8)$, $c=3.5243(9)$
Unit cell volume, (Å^3)	28.84(4)	28.46(1)	28.43(2)	28.58(2)
Z		1		
Calculated density, (g/cm^3)	2.588	2.601	2.595	2.567
Absorption correction type		Analytical		
Absorption coefficient (mm^{-1})	0.585	0.577	0.573	0.563
$F(000)$	22	21	21	21
Crystal size (mm)	$0.45 \times 0.20 \times 0.05$	$0.34 \times 0.21 \times 0.05$	$0.56 \times 0.25 \times 0.03$	$0.47 \times 0.27 \times 0.04$
Θ range for data collection (deg)	5.79–27.72	5.80–35.02	5.79–37.26	5.79–36.38
Limiting indices	$-3 \leq h \leq 3$, $-3 \leq k \leq 3$, $-4 \leq l \leq 4$	$-4 \leq h \leq 4$, $-4 \leq k \leq 4$, $-5 \leq l \leq 5$	$-5 \leq h \leq 5$, $-5 \leq k \leq 5$, $-5 \leq l \leq 6$	$-5 \leq h \leq 5$, $-5 \leq k \leq 5$, $-5 \leq l \leq 5$
Reflections collected/unique	407/25, $R_{int}=0.0543$	478/44, $R_{int}=0.0268$	1241/47, $R_{int}=0.0367$	509/46, $R_{int}=0.0285$
Max. and min. transmission	0.934 and 0.707	0.942 and 0.759	0.963 and 0.729	0.949 and 0.681
Refinement method		Full-matrix least-squares on F^2		
Data/restraints/parameters	25/0/6	44/0/6	47/0/6	46/0/6
Goodness of fit on F^2	1.300	1.259	1.285	1.290
Final R indices $[I>2\sigma(I)]$	$R_1=0.0245$, $wR_2=0.0700$	$R_1=0.0343$, $wR_2=0.0895$	$R_1=0.0254$, $wR_2=0.0649$	$R_1=0.0376$, $wR_2=0.1015$
R indices (all data)	$R_1=0.0245$, $wR_2=0.0700$	$R_1=0.0356$, $wR_2=0.0906$	$R_1=0.0274$, $wR_2=0.0654$	$R_1=0.0395$, $wR_2=0.1023$
$\Delta\rho_{max}$ and $\Delta\rho_{min}$, (e/Å^3)	0.160 and -0.289	0.292 and -0.438	0.276 and -0.234	0.368 and -0.426

in the a^*b^* plane of the reciprocal space [Figs. 3(a) and 3(b)]. Such anisotropic broadening of reflections indicates disorder. For the Li-substituted crystal, this elongation is smaller [Fig. 3(b), bottom picture] than that for the unsubstituted MgB_2 [Fig. 3(a), bottom picture]. Unsubstituted MgB_2 crystals usually are deficient in Mg by about 2–4%. Most probably Li fills Mg vacancies and, thus, the crystals are ordered better. The as-grown Li and C co-substituted crystals show very broad (002) reflections [Fig. 3(c)], most likely due to disorder. These reflections became narrower when the crystals were annealed for 2 h *in situ* (just after crystal growth) at 30

kbar and 1800 °C [Fig. 3(d)]. The reflection profiles are similar to those obtained for the unsubstituted and Li-substituted nonannealed crystals [Figs. 3(a) and 3(b)]. This observation is consistent with the behavior of the superconducting transition width ΔT_c, which for unsubstituted, Li substituted, and annealed Li-C co-substituted crystals is much smaller than ΔT_c for as-grown $Mg_{0.89}Li_{0.11}B_{1.88}C_{0.12}$, indicative of strong disorder in the last case. Thus, the study of the physical properties of the substituted MgB_2 crystals requires particular attention to the thermal treatment in the final stage of synthesis.
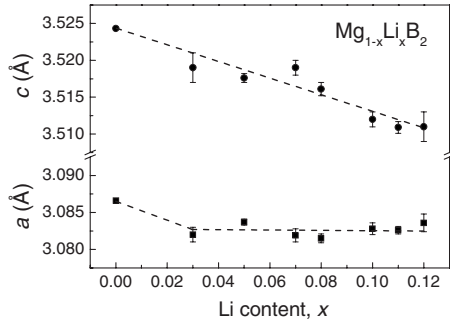
FIG. 2. Lattice parameters a and c as a function of Li content in Mg$_{1-x}$Li$_x$B$_2$ crystals.

B. Magnetic investigations

Figure 4 shows the normalized diamagnetic signal in the vicinity of T_c for Mg$_{1-x}$Li$_x$B$_2$ crystals with various Li content. The superconducting transition temperature was determined from the magnetic moment measured in a 0.5 mT dc field, after zero field cooling. The effective transition temperature T_c was defined as illustrated in Fig. 4. In Fig. 5, this temperature is plotted as a function of the Li content. For a substitution level up to 8%, T_c decreases slightly, which may correspond to filling of the Mg vacancies. Above 8% Li, a sharp drop of T_c is observed, suggestive of the appearance of
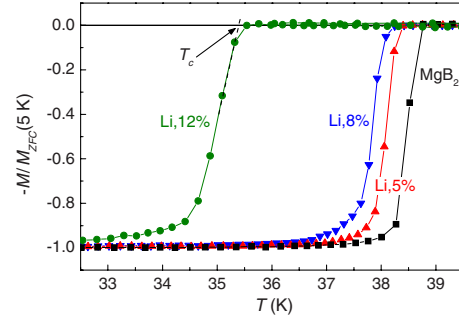
FIG. 4. (Color online) Normalized diamagnetic moment M vs temperature for the Mg$_{1-x}$Li$_x$B$_2$ single crystals with various Li content. The measurements were performed in a field of 0.5 mT, after cooling in a zero field. The superconducting transition temperature T_c is marked with an arrow.

new structural defects and increased interband scattering. As we mentioned previously, it is possible that both Li atoms and Mg vacancies are present on Mg sites. Such Mg vacancies can cause (additional) hole doping in MgB$_2$ crystals as each Mg atom contributes two electrons. Adding two holes, a Mg vacancy can have a doping effect of two Li atoms. In order to investigate the influence of Mg vacancies on T_c, additional experiments have been done. MgB$_2$ unsubstituted crystals have been annealed in vacuum at 800, 850, 875, 900,
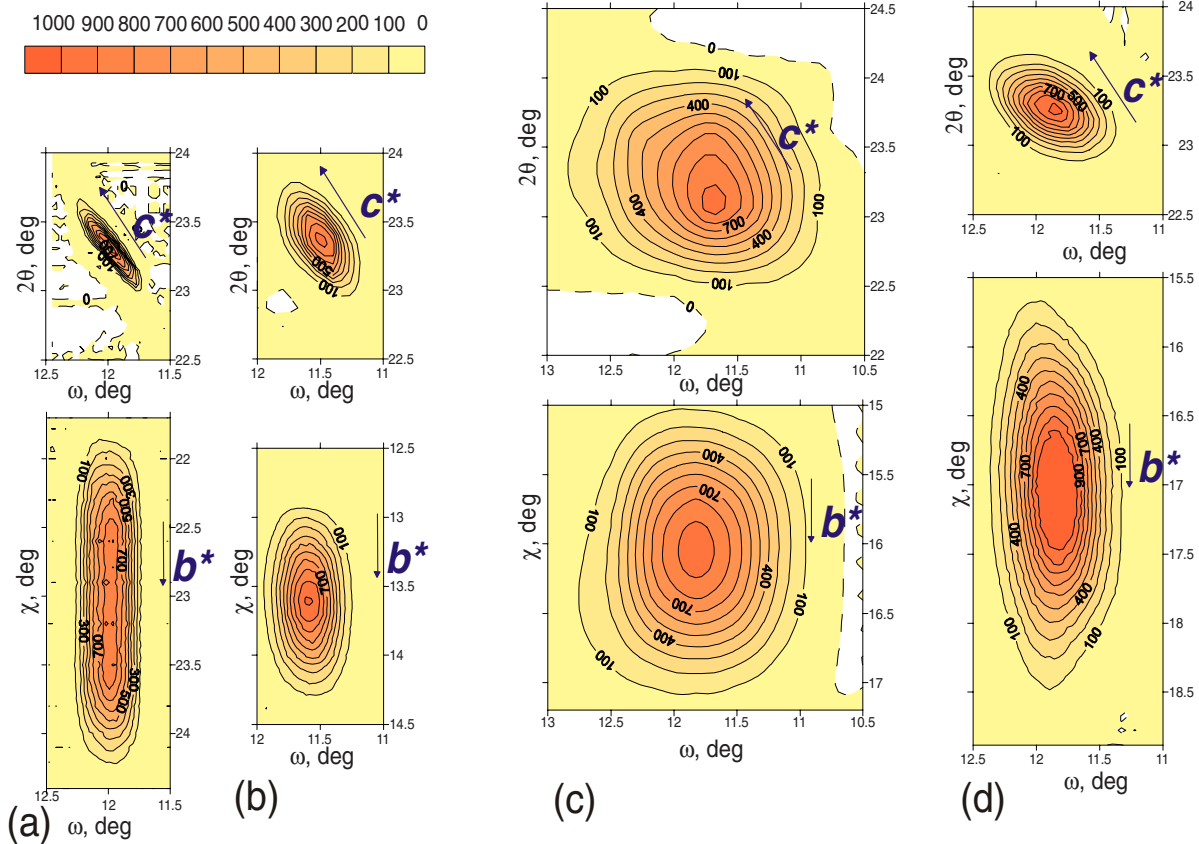
FIG. 3. (Color online) Upper pictures: $\omega-\theta$ scan of the (002) reflections; c^* is parallel to the reflection and a^*b^* is perpendicular to the plane. Lower pictures: $\omega-\chi$ scan of the (002) reflection; c^* is perpendicular to the plane, a^*b^* is parallel to the plane, and b^* is parallel to the reflection. (a), (b), (c), and (d) concern MgB$_2$, Mg$_{0.89}$Li$_{0.11}$B$_2$, Mg$_{0.89}$Li$_{0.11}$B$_{1.88}$C$_{0.12}$, and Mg$_{0.90}$Li$_{0.10}$B$_{1.85}$C$_{0.15}$ annealed at 1800 °C for 2 h after crystal growth, respectively. The scale is the same in all figures.
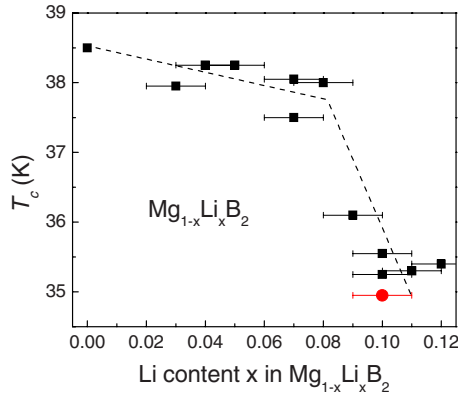
FIG. 5. (Color online) Superconducting transition temperature T_c as a function of the Li content in $Mg_{1-x}Li_xB_2$ single crystals: ■ as-grown, ● annealed in high pressure at 1800 °C.

FIG. 6. (Color online) Superconducting transition temperature T_c for MgB_2 with various substitutions.[20–22] Aluminum and carbon introduce electrons and Li^{+1} holes. Isovalent Mn^{+2} is a magnetic ion.

950, and 975 °C in order to obtain crystals with various amount of Mg vacancies and, thus, possibly with various T_c's. For the annealing temperature of 975 °C, the crystals show partial decomposition and the Mg site occupancy decreased from the as-grown 0.98 to 0.92. Surprisingly, these crystals show an unchanged T_c of 38.7 K. This means that Mg vacancies alone cannot influence T_c and the reduction in T_c is caused by the Li substitution. As we will show later, the reduction in T_c with Li substitution is caused by increased impurity scattering rather than by hole doping. One can expect that appropriate annealing of the Li-substituted crystals improves the structure and increases T_c. In order to investigate this possibility, one batch of crystals has been annealed *in situ* at 30 kbar and 1800 °C for 2 h. The results show that the high-pressure high-temperature annealing does not increase the T_c's of those crystals (see Fig. 5). This indicates that if structural defects are the main reason for the observed reduction in T_c in the Li-substituted crystals, the annealing is unable to remove them. Surprisingly, the Li-C co-substituted crystals behave in a different way. This we discuss in the paragraphs on the scattering effects.

The suppression of T_c with various substitutions in MgB_2 single crystals is shown in Fig. 6.[20–22] For the Li, C, Al, and Fe substitutions, the suppression is small or moderate. For the Mn substituted crystals, T_c decreases much more rapidly because of the magnetic pair breaking effect. The initial rate of the T_c suppression changes from about 0.1 K/%Li to about 1.2 K/%Fe, for Li and Fe substitutions, respectively. In the MgB_2 crystals co-substituted with Li and C, one can expect that hole doping with Li will compensate the effect of electron doping with C. Thus, T_c for $Mg_{1-x}Li_x(B_{1-y}C_y)_2$ may increase in comparison with T_c for $Mg(B_{1-y}C_y)_2$ with the same or similar C content. In order to verify that, three sets of substituted crystals were investigated. For two of them, the crystals were substituted separately with one element only, i.e., with C for B and with Li for Mg. For one set, the crystals were co-substituted with C and Li simultaneously. The crystals co-substituted with C and Li have lower T_c than the crystals single substituted with the same amount of C. For example, if we compare the crystal with 6% of C and the crystal with 6% of C and 11% of Li, we will find a difference in T_c of about 3.3 K (see Fig. 7). A similar difference in T_c
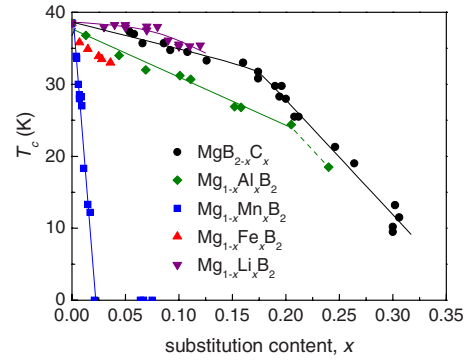
appears between the unsubstituted and 12%-Li-substituted crystals (see Fig. 4).

In order to draw more extended picture for the influence of C and Li contents on T_c, we have investigated crystals with much different substitution levels. Figure 8 shows a summary of our results for the C-Li co-substituted crystals, where the C content ranges from 2 to 9% and the Li content varies from 4 to 12%. In the whole range of substitutions, T_c is lower for C-Li co-substituted than for C only substituted crystals. The dashed lines connect the results for crystals with a similar amount of Li and with various C contents. The similar amount of Li substituted into $Mg(B_{1-x}C_x)_2$ crystals leads to the similar decrease of their T_c, even for the crystals with much different carbon content. This is not the case for the crystals single substituted with Li, where substitution up to 8% of Li changes T_c only very little.

The results indicate that even significant changes in the carrier concentration expected due to holes introduced by Li do not counterbalance the decrease of T_c caused by the C substitution. This we explain assuming that the holes occupy almost exclusively the π band and, thus, cannot compensate the C-donated electrons, which fill the σ band.[35] It is well known that in MgB_2, mostly the σ band is responsible for superconductivity, and the moderate electron or hole doping of the π band should not affect T_c. What might be the reason
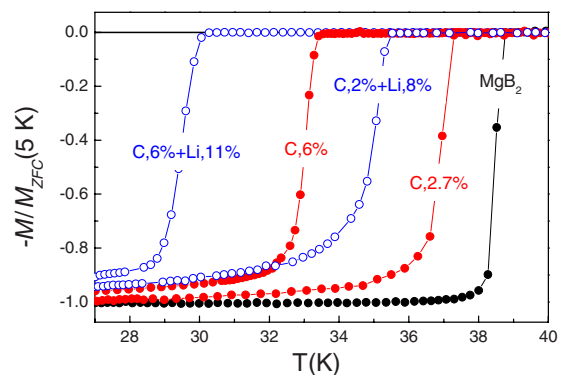
FIG. 7. (Color online) Normalized magnetic moment M vs temperature for crystals of MgB_2 substituted with C and co-substituted with C and Li.
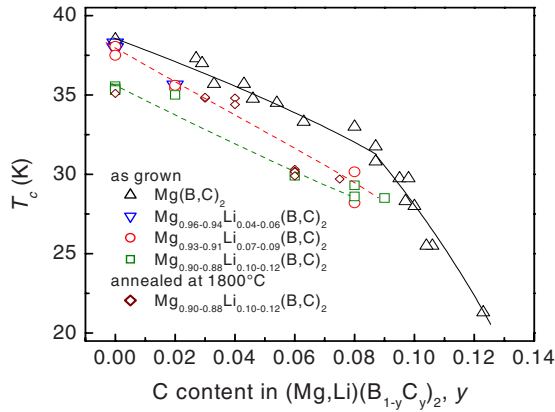
FIG. 8. (Color online) T_c suppression in C substituted crystals. Triangles: C substitution; inverted triangles, circles and squares: (Mg,Li)(B,C)$_2$, and diamonds: (Mg,Li)(B,C)$_2$ annealed under high pressure at 1800 °C. Dashed lines: crystals with the same Li content and various C content.

for suppression of T_c with the Li substitution? The observed decrease can be caused most likely by an enhanced scattering due to defects introduced by substitution and due to distortion of the lattice. To test this hypothesis, the before mentioned high-pressure high-temperature annealing has been performed (*in situ*) for the (Mg,Li)(B,C)$_2$ crystals co-substituted with 10–12% of Li and with various content of C. We expected that in this way, the lattice defects would be reduced and T_c would increase. In fact, as one can see in Fig. 8, the annealed crystals with C content $y=0.03$ and 0.04 show T_c's enhanced to values similar to those observed for the MgB$_2$ crystals substituted with C only. For higher C content, $y=0.06-0.08$, this effect is small, if any, which indicates that for larger C substitution the Li-introduced lattice distortion is much more robust and annealing resistant. In order to better understand the observed behavior of the Li-C co-substituted crystals, the electronic structure of the annealed and nonannealed crystals may be investigated by STM or point contact spectroscopy.

A clear effect of substitution on lattice disorder is shown in Fig. 9 in the form of a magnetically measured width of the superconducting transition (10–90%) as a function of T_c. The single substitution with Li or C increases ΔT_c moderately, however, the co-substitution with Li-C results in a huge increase of the transition width from 0.3 K (unsubstituted MgB$_2$) to about 8 K for the crystal with 10% of Li and 7.5% of C. This large ΔT_c is drastically reduced to about 1 K for a crystal with a similar amount of Li and C (11 and 6%, respectively), annealed *in situ* at high pressure and high temperature. This reduction in ΔT_c reflects the improved ordering of the lattice structure and is consistent with the sharpening of the (002) reflection observed for the annealed crystal with a similar amount of Li and C [see Fig. 3(d)]. As mentioned above, the annealing does not influence much the superconducting properties of the single-substituted crystals, as shown in Fig. 9 for the crystal with 10% of Li.

The upper critical field H_{c2} has been determined from magnetic moment measurements, $M(T)$ or $M(H)$, with a field oriented parallel to the *ab* plane, $H^{\|ab}$, or parallel to the *c*

axis, $H^{\|c}$. Figure 10 shows two examples of $M(T)$ dependences for $H=0.3$ and 2.5 T. The difference between T_c and $T_{c,\mathrm{on}}$ increases slightly with increasing field, but usually it does not exceed 1 K. Sets of the data similar to these presented in Fig. 10 were used to construct the H_{c2}-T phase diagram. Figure 11 shows the phase diagram for two MgB$_2$ crystals substituted with Li and, for comparison, for an unsubstituted crystal. These results clearly show that $H_{c2}^{\|ab}$ decreases with increasing Li content while $H_{c2}^{\|c}$ does not change significantly. Thus, the resulting upper critical field anisotropy $\gamma=H_{c2}^{\|ab}/H_{c2}^{\|c}$ decreases. Both Al and Li substitute Mg, therefore, one can expect an increased intraband scattering in the π band rather than in the σ band. This can be the reason why $H_{c2}(T)^{\|ab}$ decreases and $H_{c2}(T)^{\|c}$ does not change significantly. The unchanged $H_{c2}(T)^{\|c}$ might be caused by a slightly increased intraband scattering rate in the π band, which compensates the decrease. As we will show in the next chapter, resistivity increases with Li substitution, which indicates increased scattering in the π band.

Temperature dependences of H_{c2} for Li and for Al substituted crystals are shown in Fig. 12. The crystals with similar T_c show an almost identical H_{c2}-slope at T_c and a similar

FIG. 9. (Color online) Broadening of the superconducting transition ΔT_c with decreasing T_c for the MgB$_2$ crystals: unsubstituted, single substituted with Li and C, co-substituted with Li-C, and co-substituted with Li-C and annealed in high pressure at 1800 °C.
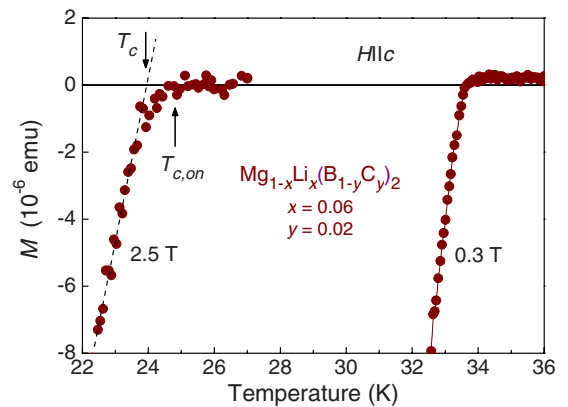
FIG. 10. (Color online) Temperature dependence of magnetic moment M in $\mu_0 H=0.3$ and 2.5 T parallel to the *c* axis of the Mg$_{0.94}$Li$_{0.06}$(B$_{0.98}$C$_{0.02}$)$_2$ crystal in the vicinity of T_c. T_c and $T_{c,\mathrm{on}}$ correspond to the transition temperature and to the temperature of the transition onset, respectively.
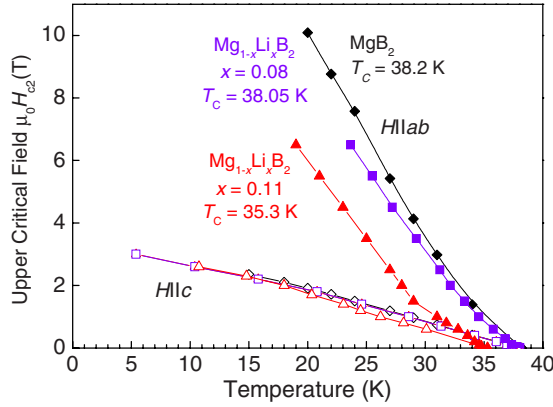
FIG. 11. (Color online) Upper critical field for two MgB$_2$ crystals substituted with 8 and 11% of Li, compared with the upper critical field for an unsubstituted crystal.

$H_{c2}(T)$ dependence despite of much different substitution levels for different substitutes. This indicates that the mechanism, which controls H_{c2}, is very similar to that one which determines T_c for both Li and Al single-substituted crystals.

The upper critical field for the Li-C co-substituted and Li or C single-substituted MgB$_2$ crystals is shown in Fig. 13. For H parallel to the ab plane, significantly different amounts of the co-substituted and single-substituted C (2 and 5%, respectively) result in similar T_c and a similar $H_{c2}(T)$ dependence. This is somewhat surprising because Li, when single-substituted up to 8%, influences both T_c and $H_{c2}(T)$ only very little (see Fig. 11). Thus, for the co-substituted crystals Mg$_{1-x}$Li$_x$(B$_{1-y}$C$_y$)$_2$, the influence of Li is much more significant. A crystal with $x=0.06$ and $y=0.02$ has $T_c=35.2$ K while $T_c=37$ K is expected for Mg(B$_{1-y}$C$_y$)$_2$ with $y=0.02$. Such a change of T_c from 37 to 35 K due to the substitution of only 6% of Li indicates that additional structural defects appear in the co-substituted samples, which can be annealed. Full explanation of the effect of Li doping would require the knowledge in other relevant parameters such as the density of states, coupling, phonon frequency, and interband scatter-
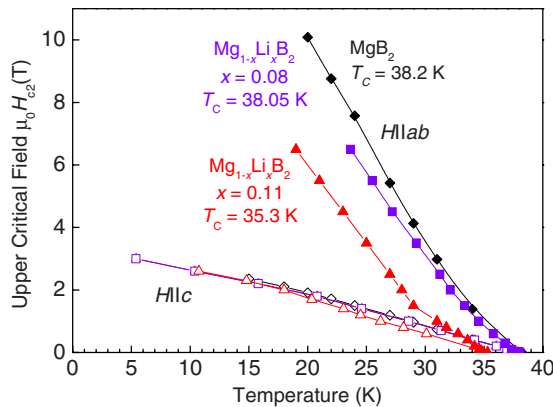
FIG. 12. (Color online) The upper critical field for Al and Li-substituted crystals. Crystals with similar T_c (but different substitution level) show a similar dH_{c2}/dT slope at T_c and slightly different $H_{c2}(T)$ dependence. Data for Al substituted crystals have been taken from Ref. 21.
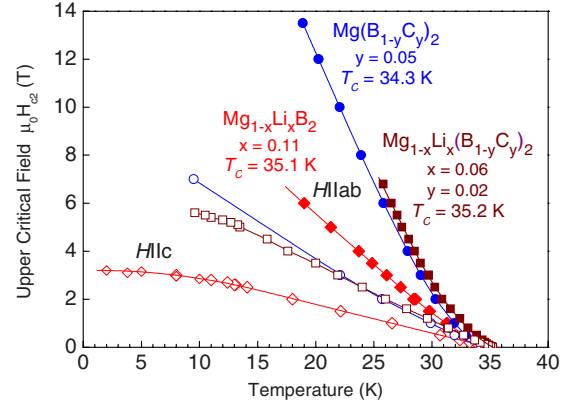
FIG. 13. (Color online) Upper critical field versus temperature for co-substituted Mg$_{1-x}$Li$_x$(B$_{1-y}$C$_y$)$_2$ and single-substituted Mg$_{1-x}$Li$_x$B$_2$ crystals.

ing, which cannot be determined in the present work. In the future, investigations of gap values are planned, which may bring more information about the mechanism of suppressing superconductivity in Li-substituted MgB$_2$.

C. Electrical transport measurements

The normalized ab-plane resistance $R(T)/R(300$ K$)$ is shown in Fig. 14. One of the co-substituted crystals has been annealed *in situ* in high pressure (30 kbar) at 1800 °C, as described above. In the same figure, the normalized $R(T)$ results obtained for MgB$_2$ and for C-substituted MgB$_2$ are also shown for comparison. The normalized resistance increases with increasing substitution level, so introduction of Li into the structure increases the charge carriers scattering. This effect is evident in the case of both the Li substituted and Li-C co-substituted crystals. A similar trend can be noticed from Fig. 15 where the absolute values of the resistivity are plotted as a function of temperature. The residual resistivity ρ_0 increases from ~ 1.2 $\mu\Omega$ cm for unsubstituted MgB$_2$ up to ~ 5.6 $\mu\Omega$ cm for the Li-substituted crystal, indicating an increasing amount of defects and thus, larger disorder. For Mg$_{1-x}$Li$_x$(B$_{1-y}$C$_y$)$_2$ with $x=0.06$ and $y=0.02$, ρ_0 is ~ 8.9 $\mu\Omega$ cm. A similar value of ρ_0 (~ 8.3 $\mu\Omega$ cm) has been obtained for the crystal with much larger Li content $x=0.12$ ($y=0.03$), when the crystal has been annealed *in situ* at high pressure and temperature. For Mg$_{1-x}$Li$_x$(B$_{1-y}$C$_y$)$_2$ with $x=0.09$ and $y=0.08$, ρ_0 increases up to ~ 22 $\mu\Omega$ cm. In the same figure, the resistivity of C-substituted crystals with $y=0.05$ ($\rho_0 \sim 9.9$ $\mu\Omega$ cm) and $y=0.083$ ($\rho_0 \sim 13$ $\mu\Omega$ cm) are shown for comparison. The uncertainty in the estimation of the resistivity due to the geometrical factor is about 15%.

A simple comparison between crystals substituted with 8.3% of C and co-substituted with 8% of C and 9% of Li shows that the crystals with similar amount of C can have a much different resistivity when additionally substituted with Li. This means that even for the strongly defected crystals, the substitution of Li further increases the amount of defects significantly. Furthermore, the comparison of resistivities for the crystal with $x=0.06$ and $y=0.02$ and for the crystal with $x=0.12$ and $y=0.03$ annealed at high pressure and tempera-
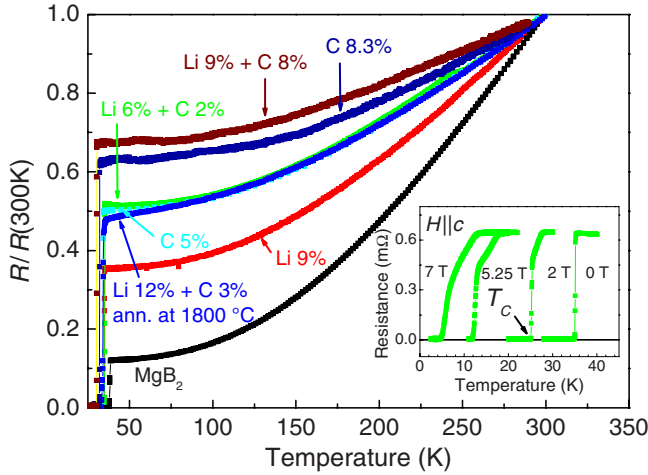
FIG. 14. (Color online) Normalized in-plane resistance $R/R(300$ K) as a function of temperature for the single crystals of $Mg_{1-x}Li_xB_2$ and $Mg_{1-x}Li_x(B_{1-y}C_y)_2$. The crystal with $x=0.12$ and $y=0.03$ has been annealed at high pressure at 1800 °C. Data for MgB_2 and $Mg(B_{1-y}C_y)_2$ with $y=0.05$ and $y=0.083$ are shown for comparison. Inset: superconducting transitions measured at various magnetic fields for the single crystal co-substituted with 6% of Li and 2% of C. The critical temperature T_c is indicated by an arrow.

ture, shows that a significantly different Li content (6 and 12%) may result in very similar ρ_0 if the crystal with the larger amount of Li is tempered. This indicates that, at least for a particular C content, the disorder introduced by Li can be removed by annealing. Relaxation effects manifest themselves also in the fact that due to the annealing, T_c increases and ΔT_c decreases, as shown in Figs. 8 and 9, respectively.

The in-plane resistance of the crystal substituted with 6% of Li and 2% of C is shown in the inset of Fig. 14 for several values of H oriented parallel to the c axis. The sharp resistive transition observed in $H=0$ gradually broadens with increas-
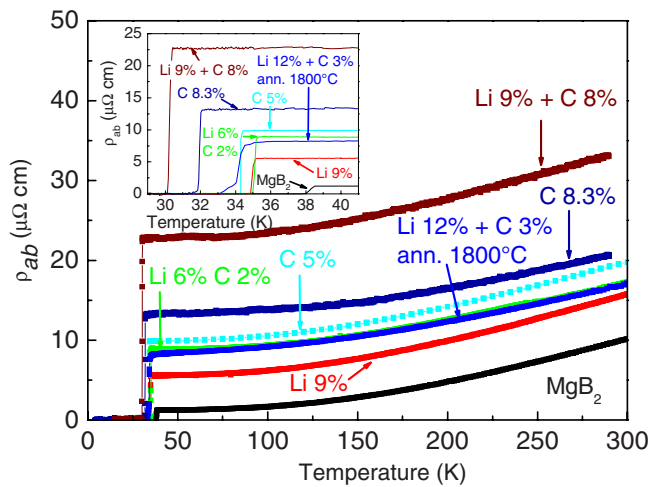
FIG. 15. (Color online) In-plane resistivity as a function of temperature for single crystals of $Mg_{1-x}Li_xB_2$ and $Mg_{1-x}Li_x(B_{1-y}C_y)_2$. The crystal with $x=0.12$ and $y=0.03$ has been annealed at high pressure at 1800 °C. Data for pure MgB_2 and for $Mg(B_{1-y}C_y)_2$ are shown for comparison. Inset: the in-plane resistivity in the vicinity of the superconducting transition.
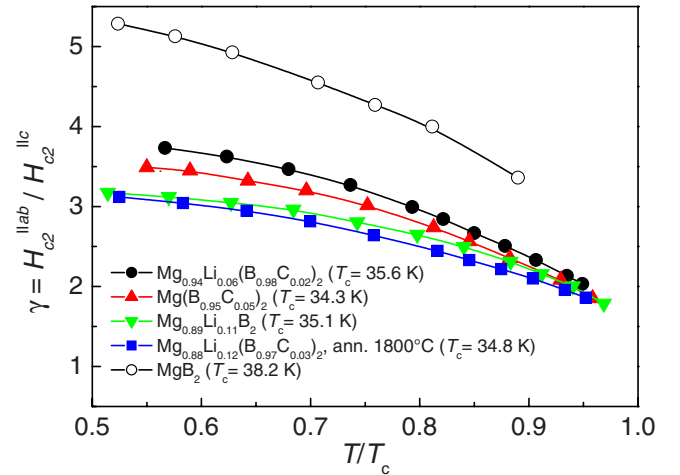
FIG. 16. (Color online) Temperature dependence of the upper critical field anisotropy γ for crystals with various substitutions and similar T_c (shown in parenthesis) in comparison with unsubstituted MgB_2.

ing field showing a two-step-like characteristics. Such a behavior has been previously observed for unsubstituted[43–45] and C-substituted[20] MgB_2, and it has been related to surface effects.[43] Therefore (but also for practical reason), we define T_c as the temperature where the resistivity vanishes (see Fig. 14). This definition is in good agreement with the one employed in the bulk property studies on pure MgB_2.[6,43,46,47] The resistivity measurements have been used to obtain the temperature dependence of H_{c2} for $H\|ab$ plane and $H\|c$ axis. For $Mg_{1-x}Li_x(B_{1-y}C_y)_2$ with $x=0.06$ and $y=0.02$, the H_{c2} has been derived from both magnetization and resistivity data and these results agree well with each other.

The $H_{c2}(T)$ curves obtained from both electrical transport and magnetic measurements have been used to evaluate the H_{c2} anisotropy $\gamma=H_{c2}^{\|ab}/H_{c2}^{\|c}$ (Fig. 16). The anisotropy decreases with increasing temperature for all compositions and it is largest for unsubstituted MgB_2. Furthermore, at lower temperatures, γ monotonically decreases with increasing doping. With increasing substitution, the anisotropy is reduced. A detailed analysis of γ involves both interband and intraband scattering processes. The main parameter determining γ is the interband coupling which influence the changes from low values at low temperatures (σ-band dominated region) to higher values at temperatures closer to T_c (mixed σ- and π-bands region).[48] This interband coupling, when weak as in MgB_2, influences the H_{c2} anisotropy much more at higher temperatures. For all substituted crystals, a smaller decrease of γ is observed at $T/T_c=1$ than at $T/T_c=0.5$ (see Fig. 16).

IV. CONCLUSIONS

Modifications of electronic properties by doping seem to be very helpful in understanding MgB_2. The substitution of Li^{+1} for Mg^{+2} introduces holes and leads to the decrease of T_c at a lower rate (~ 0.1 K/%Li) than the substitution of C for B (~ 0.7 K/%C), which introduces electrons. Co-substitution with Li and C decreases T_c more than in the case

where only C is substituted. A possible reason for this might be that holes introduced by Li occupy mainly the π band and do not compensate electrons introduced by C, which fill the σ band. The slow decrease of T_c with Li substitution up to 8% has been tentatively ascribed to the filling of Mg vacancies. For more than 8% Li content, T_c starts to drop more rapidly which indicates the presence of new structural defects and interband scattering. In the Li and C co-substituted crystals, T_c decreases due to both charge doping and impurity scattering. Doping with C-originated electrons decreases T_c as a result of the reduction in the hole-carrier content as well as a result of the introduction of new scattering centers. Additional Li substitution leads to the appearance of new structural defects, which decrease T_c. These defects can be annealed. The present data appear not to support a simple picture of holes and electrons introduced by co-substitution to balance each other.

The normal state resistivity increases in a pronounced way with the Li and C-Li substitution, reflecting scattering on the substitution-introduced defects. The structural disorder is seen directly as an additional broadening of the x-ray diffraction peaks and a smearing out of the superconducting transition. For the crystals co-substituted with Li and C, *in situ* annealing at 1800 °C increases T_c, sharpens the transition, lowers the resistivity, and narrows the x-ray reflections.

Thus, lattice distortions appear to be a significant factor in the modification of T_c. The phase diagram T_c vs substitution is asymmetric with respect to electron and hole doping, and for the comparatively less-studied hole-doped materials, the superconducting properties are influenced mainly by disorder effects. Additional experimental studies such as thermoelectric power and Hall effect measurements are desirable to separate the influence of band filling and intraband and interband scattering. Similarly, high resolution angle-resolved photoelectron spectroscopy would provide a much needed insight too. Therefore, the investigation of substituted MgB_2 single crystals will still be the challenging topic in the future.

ACKNOWLEDGMENTS

*Corresponding author: karpinski@phys.ethz.ch

[1] J. Nagamatsu, N. Nakagawa, T. Muranaka, Y. Zenitani, and J. Akimitsu, Nature (London) **410**, 63 (2001).

[2] J. Kortus, I. I. Mazin, K. D. Belashchenko, V. P. Antropov, and L. L. Boyer, Phys. Rev. Lett. **86**, 4656 (2001).

[3] A. Y. Liu, I. I. Mazin, and J. Kortus, Phys. Rev. Lett. **87**, 087005 (2001).

[4] H. J. Choi, D. Roundy, H. Sun, M. L. Cohen, and S. G. Louie, Nature (London) **418**, 758 (2002).

[5] J. Kortus, O. V. Dolgov, R. K. Kremer, and A. A. Golubov, Phys. Rev. Lett. **94**, 027002 (2005).

[6] M. Angst, R. Puzniak, A. Wisniewski, J. Jun, S. M. Kazakov, J. Karpinski, J. Roos, and H. Keller, Phys. Rev. Lett. **88**, 167004 (2002).

[7] S. L. Bud'ko and P. C. Canfield, Phys. Rev. B **65**, 212501 (2002).

[8] L. Lyard, P. Samuely, P. Szabo, T. Klein, C. Marcenat, L. Paulius, K. H. P. Kim, C. U. Jung, H.-S. Lee, B. Kang, S. Choi, S.-I. Lee, J. Marcus, S. Blanchard, A. G. M. Jansen, U. Welp, G. Karapetrov, and W. K. Kwok, Phys. Rev. B **66**, 180502(R) (2002).

[9] R. S. Gonnelli, D. Daghero, G. A. Ummarino, V. A. Stepanov, J. Jun, S. M. Kazakov, and J. Karpinski, Phys. Rev. Lett. **89**, 247004 (2002).

[10] P. Szabó, P. Samuely, J. Kačmarčík, T. Klein, J. Marcus, D. Fruchart, S. Miraglia, C. Marcenat, and A. G. M. Jansen, Phys. Rev. Lett. **87**, 137005 (2001).

[11] P. Samuely, Z. Hol'anová, P. Szabó, J. Kačmarčík, R. A. Ribeiro, S. L. Bud'ko, and P. C. Canfield, Phys. Rev. B **68**, 020505(R) (2003).

[12] M. Iavarone, G. Karapetrov, A. E. Koshelev, W. K. Kwok, G. W. Crabtree, D. G. Hinks, W. N. Kang, Eun-Mi Choi, Hyun Jung Kim, Hyeong-Jin Kim, and S. I. Lee, Phys. Rev. Lett. **89**, 187002 (2002).

[13] M. R. Eskildsen, M. Kugler, S. Tanaka, J. Jun, S. M. Kazakov, J. Karpinski, and Ø. Fischer, Phys. Rev. Lett. **89**, 187003 (2002).

[14] M. R. Eskildsen, N. Jenkins, G. Levy, M. Kugler, Ø. Fischer, J. Jun, S. M. Kazakov, and J. Karpinski, Phys. Rev. B **68**, 100508(R) (2003).

[15] A. Gurevich, Phys. Rev. B **67**, 184515 (2003).

[16] S. C. Erwin and I. I. Mazin, Phys. Rev. B **68**, 132505 (2003).

[17] A. Bianconi, S. Agrestini, D. Di Castro, G. Campi, G. Zangari, N. L. Saini, A. Saccone, S. De Negri, M. Giovannini, G. Profeta, A. Continenza, G. Satta, S. Massidda, A. Cassetta, A. Pifferi, and M. Colapietro, Phys. Rev. B **65**, 174515 (2002).

[18] T. Masui, S. Lee, and S. Tajima, Phys. Rev. B **70**, 024504 (2004).

[19] S. Lee, T. Masui, A. Yamamoto, H. Uchiyama, and S. Tajima, Physica C **397**, 7 (2003).

[20] S. M. Kazakov, R. Puzniak, K. Rogacki, A. V. Mironov, N. D. Zhigadlo, J. Jun, Ch. Soltmann, B. Batlogg, and J. Karpinski, Phys. Rev. B **71**, 024533 (2005).

[21] J. Karpinski, N. D. Zhigadlo, G. Schuck, S. M. Kazakov, B. Batlogg, K. Rogacki, R. Puzniak, J. Jun, E. Müller, P. Wägli, R. Gonnelli, D. Daghero, G. A. Ummarino, and V. A. Stepanov, Phys. Rev. B **71**, 174506 (2005).

[22] K. Rogacki, B. Batlogg, J. Karpinski, N. D. Zhigadlo, G. Schuck, S. M. Kazakov, P. Wägli, R. Puźniak, A. Wiśniewski, F. Carbone, A. Brinkman, and D. van der Marel, Phys. Rev. B **73**, 174520 (2006).

[23] C. Krutzler, M. Zehetmayer, M. Eisterer, H. W. Weber, N. D. Zhigadlo, J. Karpinski, and A. Wisniewski, Phys. Rev. B **74**, 144511 (2006).

[24] Y. G. Zhao, X. P. Zhang, P. T. Qiao, H. T. Zhang, S. L. Jia, B. S. Cao, M. H. Zhu, Z. H. Han, X. L. Wang, and B. L. Gu, Physica C **361**, 91 (2001).

[25] S. Y. Li, Y. M. Xiong, W. Q. Mo, R. Fan, C. H. Wang, X. G. Luo, Z. Sun, H. T. Zhang, L. Li, L. Z. Cao, and X. H. Chen, Physica C **363**, 219 (2001).

[26] G. J. Xu, J.-C. Grivel, A. B. Abrahamsen, X. P. Chen, and N. H. Andersen, Physica C **399**, 8 (2003).

[27] M. Monni, C. Ferdeghini, M. Putti, P. Manfrinetti, A. Palenzona, M. Affronte, P. Postorino, M. Lavagnini, A. Sacchetti, D. Di Castro, F. Sacchetti, C. Petrillo, and A. Orecchini, Phys. Rev. B **73**, 214508 (2006).

[28] R. H. T. Wilke, S. L. Bud'ko, P. C. Canfield, D. K. Finnemore, R. J. Suplinskas, and S. T. Hannahs, Phys. Rev. Lett. **92**, 217003 (2004).

[29] V. Braccini, A. Gurevich, J. E. Giencke, M. C. Jewell, C. B. Eom, D. C. Larbalestier, A. Pogrebnyakov, Y. Cui, B. T. Liu, Y. F. Hu, J. M. Redwing, Qi Li, X. X. Xi, R. K. Singh, R. Gandikota, J. Kim, B. Wilkens, N. Newman, J. Rowell, B. Moeckly, V. Ferrando, C. Tarantini, D. Marré, M. Putti, C. Ferdeghini, R. Vaglio, and E. Haanappel, Phys. Rev. B **71**, 012504 (2005); **71**, 179902(E) (2005).

[30] M. Angst, S. L. Bud'ko, R. H. T. Wilke, and P. C. Canfield, Phys. Rev. B **71**, 144512 (2005).

[31] A. V. Sologubenko, N. D. Zhigadlo, S. M. Kazakov, J. Karpinski, and H. R. Ott, Phys. Rev. B **71**, 020501(R) (2005).

[32] D. Di Castro, M. Ortolani, E. Cappelluti, U. Schade, N. D. Zhigadlo, and J. Karpinski, Phys. Rev. B **73**, 174509 (2006).

[33] R. S. Gonnelli, D. Daghero, A. Calzolari, G. A. Ummarino, V. Dellarocca, V. A. Stepanov, S. M. Kazakov, N. Zhigadlo, and J. Karpinski, Phys. Rev. B **71**, 060503(R) (2005).

[34] P. Samuely, P. Szabó, P. C. Canfield, and S. L. Bud'ko, Phys. Rev. Lett. **95**, 099701 (2005).

[35] F. Bernardini and S. Massidda, Phys. Rev. B **74**, 014513 (2006).

[36] J. Karpinski, M. Angst, J. Jun, S. M. Kazakov, R. Puzniak, A. Wisniewski, J. Roos, H. Keller, A. Perucchi, L. Degiorgi, M. R. Eskildsen, P. Bordet, L. Vinnikov, and A. Mironov, Supercond. Sci. Technol. **16**, 221 (2003).

[37] J. Karpinski, S. M. Kazakov, J. Jun, M. Angst, R. Puzniak, A. Wisniewski, and P. Bordet, Physica C **385**, 42 (2003).

[38] CRYSALIS RED, Oxford Diffraction Ltd., Version 1.171.29.9.

[39] G. Sheldrick, *SHELXL-97: Program for the Refinement of Crystal Structures* (University of Göttingen, Germany, 1997).

[40] J. Schmidt, W. Schnelle, Y. Grin, and R. Kniep, Solid State Sci. **5**, 535 (2003).

[41] U. Burkhardt, V. Gurin, F. Haarmann, H. Borrmann, W. Schnelle, A. Yaresko, and Y. Grin, J. Solid State Chem. **177**, 389 (2004).

[42] M. Avdeev, J. D. Jorgensen, R. A. Ribeiro, S. L. Bud'ko, and P. Canfield, Physica C **387**, 301 (2003).

[43] U. Welp, A. Rydh, G. Karapetrov, W. K. Kwok, G. W. Crabtree, Ch. Marcenat, L. Paulius, T. Klein, J. Marcus, K. H. P. Kim, C. U. Jung, H.-S. Lee, B. Kang, and S.-I. Lee, Phys. Rev. B **67**, 012505 (2003).

[44] S. Lee, H. Mori, T. Masui, Y. Eltsev, A. Yamamoto, and S. Tajima, J. Phys. Soc. Jpn. **70**, 2255 (2001).

[45] M. Pissas, D. Stamopoulos, S. Lee, and S. Tajima, Phys. Rev. B **70**, 134503 (2004).

[46] A. Rydh, U. Welp, J. M. Hiller, A. Koshelev, W. K. Kwok, G. W. Crabtree, K. H. P. Kim, K. H. Kim, C. U. Jung, H. S. Lee, B. Kang, and S. I. Lee, Phys. Rev. B **68**, 172502 (2003).

[47] A. V. Sologubenko, J. Jun, S. M. Kazakov, J. Karpinski, and H. R. Ott, Phys. Rev. B **65**, 180505(R) (2002).

[48] T. Dahm and N. Schopohl, Phys. Rev. Lett. **91**, 017001 (2003).